Izvestiya, Atmospheric and Oceanic Physics, Vol. 40, No. 3, 2004, pp. 291–305. Translated from Izvestiya AN. Fizika Atmosfery i Okeana, Vol. 40, No. 3, 2004, pp. 330–346.

Estimation of Radiation, Heat, and Water Exchange between Steppe Ecosystems and the Atmosphere in the SWAP Model

E. M. Gusev*, O. N. Nasonova*, and B. P. Mohanty**

** Institute of Water Problems, Russian Academy of Sciences, ul. Gubkina 3, Moscow, 119991 Russia*
e-mail: gusev@aqua.laser.ru

*** Department of Biological and Agricultural Engineering, 301C Scoates Hall, Texas A&M University, College Station, TX 77843-2117, USA*

Received February 27, 2003; in final form, October 10, 2003

Abstract—The ability of the SWAP (Soil Water–Atmosphere–Plants) land surface model to reproduce heat and moisture transfer in natural and agricultural steppe ecosystems is examined. The study is based on hourly net radiation data, hourly turbulent sensible and latent heat fluxes, and the land surface characteristics derived in the course of the Southern Great Plains 1997 (SGP97) Hydrology Experiment performed in 1997 in prairies located in the Southern Great Plains (Oklahoma).

INTRODUCTION

Solar radiation reaching the land surface is transformed in a thin planetary layer inside the soil–vegetation (or snow cover)–atmosphere system (SVAS) [1]. Studies of the SVAS have led to the development of a number of heat and moisture transfer models ranging from the simplest parametrization schemes for atmospheric general circulation models to detailed land surface models used in land hydrology, climatology, global ecology, etc. [2]. Nevertheless, the modeling of heat and moisture transfer in the SVAS remains an important task, which is best supported by the fact that this task is still of primary importance in the international project "Biospheric Aspects of the Hydrological Cycle" (BAHC) launched as early as 1992 within the framework of the International Geosphere Biosphere Program (ICBP).

We have been developing a land surface model, namely, the SWAP (Soil Water–Atmosphere–Plants) model, for about ten years.

Due to our participation in international projects, such as the Project for Intercomparison of Land-surface Parametrization Schemes (PILPS), the Snow Model Intercomparison Project (SnowMIP), and the Rhone AGGregation experiment (Rhone-AGG), we had access to unique observation datasets, which were used to validate the SWAP model as applied to some experimental objects located in various natural zones and ranging from local to continental spatial scales [3–18]. The model was validated primarily by using hydrological characteristics (runoff, soil moisture content, snow water equivalent, etc.), while energy characteristics (net radiation, land surface radiation temperature, and sensible and latent turbulent fluxes) were used for model validation over a single year (1987) for the Cabauw experimental site (the Netherlands) [3, 9, 10]. This site is located in a temperate marine area characterized by grassland vegetation and a shallow water table. This ensures stable moistening conditions for the rooting zone, so that the soil moisture differs little from the field capacity.

It was mentioned above that land-surface models are intended not only for hydrological problems but also for climate and ecology studies. For this reason, the SWAP model should be further validated by using energy-balance components at the land surface in a wide range of natural conditions. Thus, the goal of this study is to validate the SWAP model against vertical energy fluxes measured in prairies of the Southern Great Plains (Oklahoma). The primary reason for which we chose this region was that it differs fundamentally from Cabauw, having a continental semiarid climate. This determines highly varying weather conditions, which, in conjunction with the relatively deep water table, lead to significant amplitudes of within-year oscillations in soil moistening. Moreover, the available data were use to validate the model not only for natural grassland areas (like Cabauw) but also for agricultural areas with winter wheat crops.

BRIEF DESCRIPTION OF THE SWAP MODEL

Detailed characterizations of various versions of the SWAP model can be found in [3–7, 10, 11, 13]. For this reason, we present only a brief description of the model.

A distinctive feature of the SWAP model (considered here in a version intended for treating local-scale

objects, in which case the spatial inhomogeneities of external factors and land surface characteristics can be neglected) is that it combines a relatively high physical validity, basically analytical techniques for solving the model equations (while most land surface models make use of numerical methods), and a tendency of reducing the number of model parameters.

Because analytical solution methods are used, the SWAP model has a nontraditional structure [3]. For example, the calendar year in the model is divided into a warm and a cold period (Fig. 1), for each of which there is an individual model component. The cold-period algorithm is used if the daily mean air temperature steadily passes through 0°C (toward negative values) or if the ground is covered with snow or includes a frozen layer. In the other cases, the calculations are based on the warm-period algorithm.

The warm-period component of the model describes the following processes: the interception of atmospheric precipitation by vegetation and subsequent evaporation, the division of part of the precipitation falling on the land surface into infiltration and surface runoff, water balance formation in the aeration zone (including transpiration, physical evaporation of water by the soil, water exchange with the groundwater, variations in the soil water storage), and the formation of heat balance components at the land surface and its thermal conditions.

The simulation of heat and water transfer in the cold period of the year is supplemented with equations describing the formation of the water and thermal regime for the snow cover and the freezing and thawing of the soil. Interception of atmospheric precipitation is taken into account only in the case of high plants.

The description of evaporation is based on some conclusions of A.I. Budagovskii's semiempirical theory [19], which makes use of the concepts of potential evaporation from the soil (physical evaporation from the surface of a sufficiently wet soil) and potential transpiration (transpiration of closed-canopy normally vegetating plants under sufficient moistening). The calculation of these characteristics is based on the Monin–Oboukhov similarity theory for the atmospheric surface layer with temperature and humidity stratification [20, 21].

The aeration zone in the model is divided into two layers [6]. One of them is the rooting zone, defined as the soil layer containing about 95% of the root biomass. The other layer is located between the bottom boundary of the rooting zone and the time-varying water table depth. In general, the hydraulic and physical characteristics of this layer differ from those of the rooting zone.

Modeling soil water dynamics (for both warm and cold periods) is based on the water balance equations for each aeration layer and the equations determining water transfer at their boundaries [6]. Surface runoff is formed when the intensity of rain falling on the land surface in the warm period or the rate of snow melting in the cold period exceeds the infiltration rate (Horton runoff), which is calculated by using a modified Green and Ampt model [22]. The parametrization of subsurface runoff is based on the hydraulic relationship between groundwater and streamflow [6]. In some cases (e.g., for a deep water table, when the interaction between the surface water and groundwater is insignificant), the calculation of the subsurface runoff intensity is based on the hypothesis of free drainage [5, 12]. To derive the runoff hydrograph, the model also involves feasible horizontal transformation of the calculated instant surface and subsurface runoffs within an extended object (watershed, river basin) with allowance for the so-called lag time of flow.

The initial data required for the SWAP model include actinometric and hydrometeorological observations (incoming long- and shortwave radiation, precipitation, air pressure, wind speed, air temperature and humidity) and the characteristics of the land surface. The latter include thermal, hydraulic, and physical soil parameters (porosity, soil hydraulic conductivity at saturation, soil water matric potential, etc.), vegetation characteristics (vegetation type, the leaf and stem area index, the rooting depth, the albedo of the vegetation cover, etc.), snow cover parameters (roughness length, maximum albedo of deep snow), and the morphological characteristics of the watershed surface (slope, the depth to the impermeable layer, etc.).

The set of outputs in the SWAP model that characterize the dynamics of the thermal and water regime in the ecosystem under consideration and can be used for model validation is very large. In particular, it includes heat-balance components, the land surface temperature, precipitation amounts intercepted by plants, total evaporation and its components (transpiration, evaporation from bare soil or snow, evaporation of the rainfall intercepted by plants), snow water equivalents, snow depth and density, snow melt, surface runoff, drainage, soil moisture, and the depths of frozen and thawed layers. According to our task, as outputs for comparison with observations, we primarily used flux characteristics of the radiation, thermal, and moisture conditions of ecosystems, such as reflected shortwave radiation, longwave radiation, the net radiation of the land surface, and turbulent fluxes of heat and moisture.

CHARACTERIZATION OF THE OBJECTS UNDER STUDY AND THE DATA USED

As was mentioned above, we validated the SWAP model for steppe ecosystems located on the Southern Great Plains (Oklahoma) (Fig. 2). In many respects, the choice of this region was determined by the presence of a sufficiently large (in area) experimental site, where regular actinometric, meteorological, and hydrological measurements are conducted by ground-based and remote sensing techniques on several hundreds of fields with various types of soil and vegetation. These measurements are accompanied by the determination of

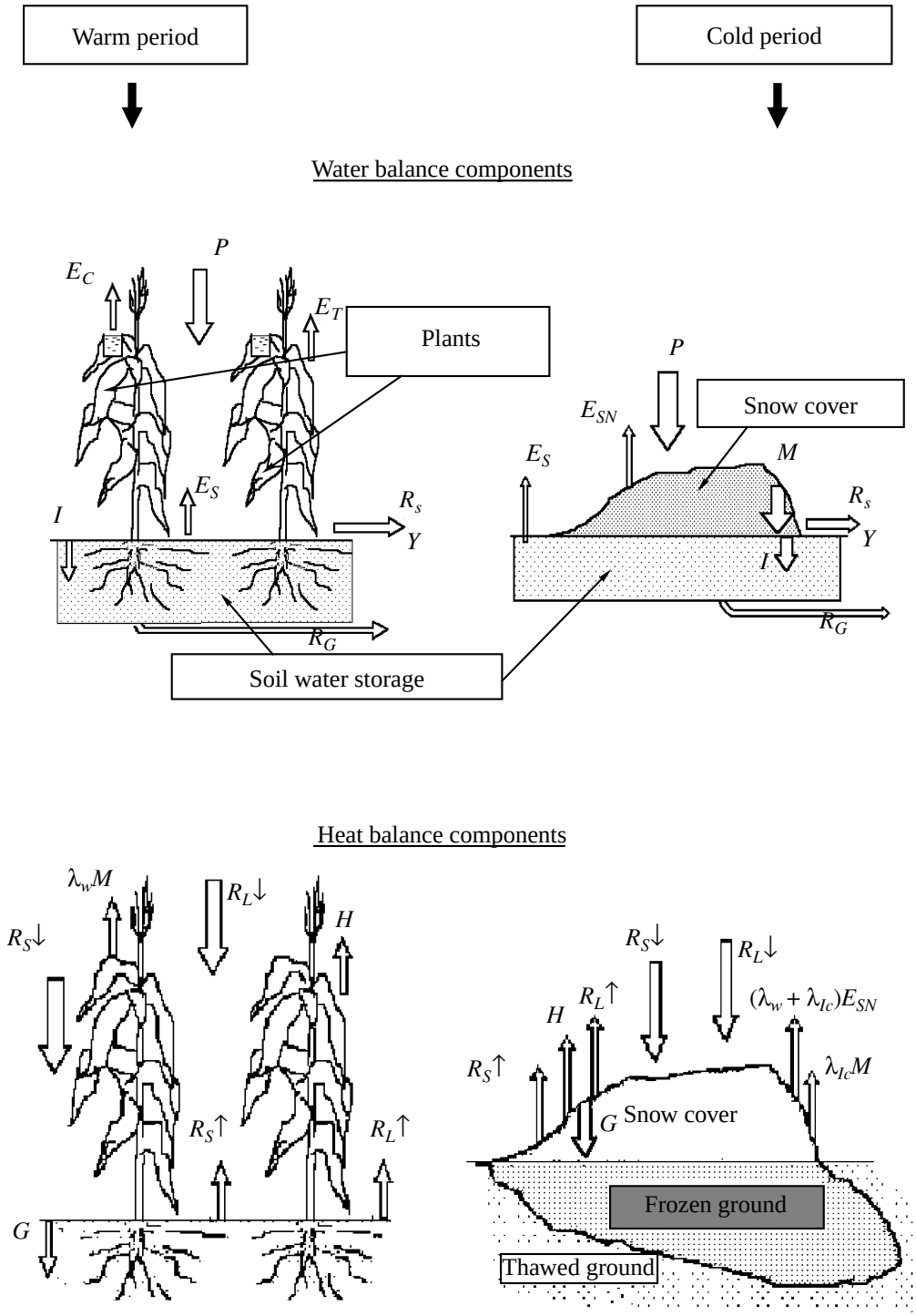

Fig. 1. Schematic diagram of the heat and moisture transfer processes described by the SWAP model in the case of low plants: P is atmospheric precipitation, E_T is transpiration, E_S is evaporation of water by the soil; E_C is evaporation of precipitation intercepted by plants, E_{SN} is evaporation of snow, $E = E_T + E_S + E_C + E_{SN}$ is the evapotranspiration, R_G is drainage, R_s is surface runoff, M is the intensity of snow melt, I is infiltration, $R_S\downarrow$ and $R_S\uparrow$ are the incoming and outgoing shortwave radiation, $R_L\downarrow$ and $R_L\uparrow$ are the incoming and outgoing longwave radiation, H is the turbulent sensible heat flux, G is the heat flux to the soil or snow cover, λ_w is the specific heat of vaporization for water, and λ_{Ic} is the specific heat of fusion for water.

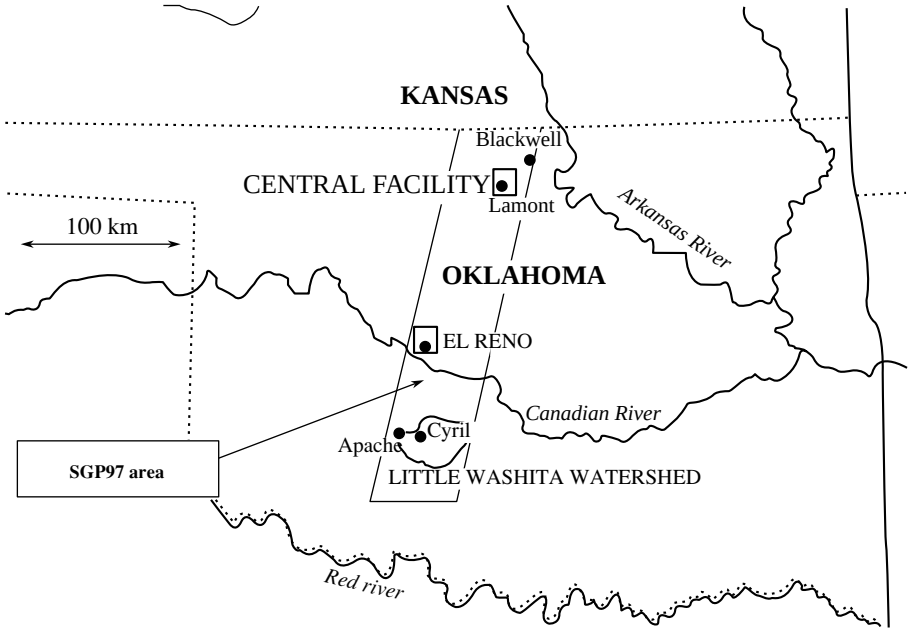

Fig. 2. Schematic map of the observation region.

soil and vegetation parameters, geomorphological characteristics, etc. This territory is covered with three research networks of geophysical observations: ARM CART (Atmospheric Radiation Measurement, Cloud and Radiation Testbed) of the US Department of Energy and the Oklahoma Mesonet and Micronet USDA-ARS (US Department of Agriculture–Agricultural Research Service) [23].

In this study, we used the data measured during the SGP97 experiment (Southern Great Plains 1997 Hydrology Experiment, see http://hydrolab.arsusda.gov/sgp97/) at six 800×800-m fields located at three experimental sites on the Southern Great Plains: (1) in the Little Washita watershed (LW02 and LW03 fields), (2) at the Agricultural Research Service facility near El Reno (ER01 and ER13 fields), and (3) at the ARM CART Central Facility near Lamont (CF01 and CF02 fields) (Fig. 2).

Various soil parameters (density, texture, the relationships of the matric potential and hydraulic conductivity with soil moisture) and vegetation parameters (rooting depth, leaf area index) were determined for each of these fields during the SGP97 intensive observation period from June 18 to July 18, 1997. Soil moisture profiles were measured by the weight method in layers from 0 to 90 cm at ER01 (July 7 and 17) and ER13 (July 8). Additionally, the net radiation, the heat flux into the soil, and atmospheric turbulent heat and water vapor fluxes—the characteristics used for model validation in this study—were measured by various experiment participants at each field over different time intervals (from 1–2 days to 1–2 months). Turbulent sensible and latent heat fluxes were measured by two techniques: eddy correlation (EC) and the energy balance Bowen ratio (EBBR). Since energy fluxes in the SGP97 were measured over rather short time intervals, the experimental data for SWAP validation were supplemented with the radiation-balance components measured over all of 1997 at the ARM CART stations nearest to the fields chosen: the Lamont station (for CF01) and the Cyril station (for LW02, LW03, and ER01). These stations and fields (unlike CF02 and ER13) had the same type of vegetation (perennial grass). For this reason, the radiation characteristics measured at the stations can be considered similar to the corresponding characteristics measured at the fields and can be used for model validation.

Since the radiation, thermal, and moisture conditions in the ecosystems chosen were simulated over all of 1997, the model needed hydrometeorological data over this period. As these data, we used the five-minute measurements of precipitation, wind speed, air humidity, temperature, pressure conducted at the Oklahoma Mesonet stations nearest to the fields: Apache for LW02 and LW03, Blackwell for CF01 and CF02, and El Reno for ER01 and ER13 (Fig. 2). The incoming long- and shortwave radiation was specified from the observations of these characteristics performed at the ARM CART stations indicated above: Lamont (for CF01 and CF02) and Cyril (for LW02, LW03, ER01, and ER13). All the observations were averaged at one-hour intervals, which corresponds to the time step used in the model.

An important element in the model is the hydraulic and physical characteristics of soil and vegetation. The hydraulic characteristics of soil include the porosity W_{sat}, the field capacity W_{fc}, the wilting point W_{wp},

and the relationships of the hydraulic conductivity K and the matric potential ϕ with the soil moisture W. The functions $K(W)$ and $\phi(W)$ are described by using the Clapp and Hornberger parametrizations [24], which require the soil matric potential at saturation ϕ_0, the Clapp–Hornberger parameter B, and the hydraulic conductivity at saturation K_0.

In this work, the soil parameters were taken the same for both aeration layers. The predictors for soil parameter determination were the profile-averaged bulk density and soil texture data (the sand, silt, and clay percentages according to the three-component classification of soil particle sizes accepted at the National Soil Protection Service of the US Department of Agriculture (USDA-SCS) [25]) obtained by analyzing soil samples taken from each field. These data and the Rosette neural network software program [26] developed at the USDA Salinity Laboratory were used to estimate W_{sat} and K_0 at the fields and to construct $K(W)$ and $\phi(W)$ based on van Genuchten–Mualem parametrizations [27]. Next, $\phi(W)$ and B were determined by interpolating the resulting function $\phi(W)$ with the use of the Clapp–Hornberger equation for the matric potential ranging from –33 to –1500 kPa. The soil moisture at $\phi = -1500$ kPa was used as W_{wp}.

The following procedure was used to determine W_{fc}. By definition, W_{fc} is the water content reached by fully saturated soil in 1–3 days as a result of free redistribution of water over the soil profile [28]. Water redistribution in the soil after saturation can also be simulated theoretically by solving the Richardson equation for hydraulic conductivity [29] if $\phi(W)$ and $K(W)$ are available. This method was used in our study. As a result, the field capacity was set equal to the average soil moisture in a one-meter layer obtained by simulating water redistribution in the soil profile two days after saturation. The soil moisture was calculated by solving the equation for hydraulic conductivity (with the help of the HYDRUS-1 software program also developed at the Salinity Laboratory [29]) with the use of the resulting $\phi(W)$ and $K(W)$ described by van Genuchten–Mualem parametrizations. The soil characteristics calculated for six fields are listed in Table 1.

The most difficult task was to determine vegetation characteristics, primarily, to recover the annual cycles of the leaf area index (LAI) and the leaf and stem area index (LSAI) for winter wheat and perennial grass, because these characteristics (and some others) were measured at each field only during an intensive observation period once a year. The dynamics of the LSAI for winter wheat was simulated by using the technique proposed in [30]. Following this technique, the increase in the LSAI is determined by temperature and water factors and can be estimated at every moment of time from the sums of accumulated positive daily mean air temperatures $\Sigma T_{>0}$ and the water stress function reflecting the nonoptimality of the moisture conditions for vegetation. In the case of sufficient moistening, i.e., when the water storage V of the rooting zone exceeds a critical value V_{cr} (where V_{cr} is a threshold above which the soil moisture is no longer a limiting factor for plant transpiration [19]), the LSAI dynamics is determined only by the temperature factor. Unfortunately, regular field measurements of soil water storage were not conducted (the characteristic investigated in the SGP97 experiment and related to the soil water regime was primarily the soil moisture in the 0–5 cm layer). That is why the moisture conditions can be judged only from indirect features, namely, from the precipitation amount and the precipitation distribution over the year. An analysis of the 1997 data has suggested that moistening in the area under study can be regarded as sufficient, at least, over most of the year. That is why the simulation of the LSAI dynamics was based only on $\Sigma T_{>0}$. Next, the leaf area index was determined by using the empirical relations between LSAI and LAI [31]. The simulated monthly means of LAI and LSAI are listed in Table 1.

The LSAI values for grass were constant over the year and were equal to their SGP97 measured values. The annual cycle of the LAI was specified approximately, based on the authors' experience, provided that the July LAI values corresponded to the observations. Unfortunately, the lack of phytometric data prevented us from taking into account the reduction in the LAI and LSAI caused by pasturing.

Since the albedo of perennial grass varies little over the year, it was set equal to a constant of 0.23 typical for grass. The albedo of winter wheat depends on the growth stage. Since there were no phenological field observations during the year, the dates corresponding to various growth stages for winter wheat were approximately estimated from $\Sigma T_{>0}$ [30], after which the albedo corresponding to a growth stage was approximately determined from literature [32, 35]. The monthly mean albedo values for two wheat-covered fields are listed in Table 1.

The transpiration parameter describing the deviation of actual transpiration from its potential value depending on the growth stage [19] (Table 1) was approximately determined by using expert estimates based on the authors' experience [7].

According to the measurements, the rooting depth was set equal to 70 cm for winter wheat and 100 cm for perennial grass.

Since the depth to the upper impermeable layer h_0 and the surface slope J at the field locations were not available (the available data only suggest a sufficiently deep (>3 m) water table), h_0 was set equal to 4 m, and J was specified as 0.01 [34, 35]. It should be noted that h_0 and J are only required to close the description of the ecosystem's water conditions by describing surface and subsurface runoff transformation. Since the observed and simulated runoff hydrographs for the fields under study were not compared (because of the lack of exper-

Table 1. Locations of the fields and their parameters

Location	Field	Vegetation type	Soil type	Soil parameters						Vegetation parameters by months												
				W_{sat}, m^3m^{-3}	W_{fs}, m^3m^{-3}	W_{wp}, m^3m^{-3}	K_0, mm/s	ϕ_0, mm	B	Parameter	I	II	III	IV	V	VI	VII	VIII	IX	X	XI	XII
Little Washita	LW02	1*	1**	0.35	0.30	0.07	0.0022	–620	3.2	LAI / LSAI	0.2 / 1.9	0.1 / 1.9	0.2 / 1.9	0.5 / 1.9	1.1 / 1.9	1.4 / 1.9	1.6 / 1.9	1.4 / 1.9	1.2 / 1.9	0.9 / 1.9	0.4 / 1.9	0.2 / 1.9
Little Washita	LW03	1*	3**	0.40	0.29	0.05	0.0071	–51	4.1		0.2 / 1.9	0.1 / 1.9	0.2 / 1.9	0.5 / 1.9	1.1 / 1.9	1.4 / 1.9	1.6 / 1.9	1.4 / 1.9	1.2 / 1.9	0.9 / 1.9	0.4 / 1.9	0.2 / 1.9
El Reno	ER01	1*	2**	0.42	0.33	0.09	0.0018	–690	3.2		0.3 / 3.6	0.3 / 3.6	0.4 / 3.6	0.8 / 3.6	1.8 / 3.6	2.5 / 3.6	2.8 / 3.6	2.5 / 3.6	1.9 / 3.6	1.3 / 3.6	0.8 / 3.6	0.4 / 3.6
El Reno	ER13	2*	2**	0.41	0.38	0.13	0.0004	–370	5.4		0.0 / 0.0	0.2 / 0.2	0.7 / 0.7	2.0 / 3.0	1.5 / 5.0	0.2 / 3.7	0.0 / 0.9	0.0 / 0.0	0.0 / 0.0	0.0 / 0.0	0.0 / 0.0	0.0 / 0.0
Central Facility	CF01	1*	2**	0.47	0.43	0.15	0.0008	–340	5.3		0.2 / 2.0	0.1 / 2.0	0.2 / 2.0	0.5 / 2.0	1.1 / 2.0	1.4 / 2.0	1.6 / 2.0	1.4 / 2.0	1.2 / 2.0	0.9 / 2.0	0.4 / 2.0	0.2 / 2.0
Central Facility	CF02	2*	2**	0.45	0.37	0.13	0.0020	–570	3.7		0.0 / 0.0	0.2 / 0.2	0.7 / 0.7	1.9 / 2.9	1.5 / 5.0	0.2 / 3.7	0.0 / 1.3	0.0 / 0.0	0.0 / 0.0	0.0 / 0.0	0.0 / 0.0	0.0 / 0.0
	ER13, CF02									albedo	0.15	0.15	0.17	0.19	0.22	0.23	0.16	0.15	0.15	0.15	0.15	0.15
	ER01, LW02, LW03, CF01									transpiration parameter	0.3	0.4	0.6	0.8	1.0	1.0	1.0	1.0	1.0	1.0	0.5	0.3

* 1 perennial grass, 2 winter wheat; ** 1 loam, 2 silt loam, 3 loamy sand.

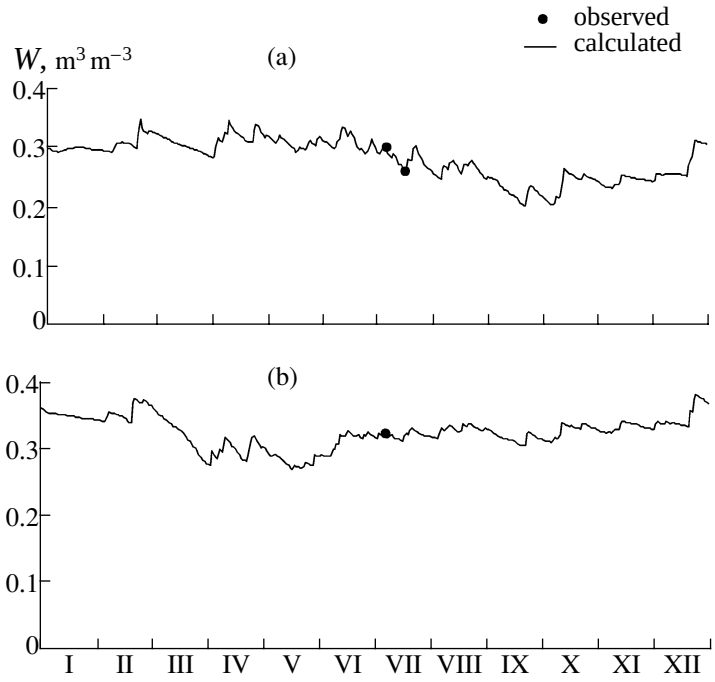

Fig. 3. Simulated dynamics of moisture in the rooting zone and the moisture values measured during the SGP97 intensive observation period at fields (a) ER01 and (b) ER13.

imental data), the parameters h_0 and J are not critical in this case. The only requirement for them was that they ensure a sufficiently deep water table such that the upward water flux to the rooting zone is virtually absent. The computations performed have shown that this requirement is satisfied in all cases for the specified values of h_0 and J.

Another type of data required for running the model over a particular time period is initial conditions, which ensure the uniqueness of the resulting solution. In the SWAP model, the initially specified quantities include soil moisture in both aeration layers, the water table depth, snow water equivalents, and the depth of frozen ground. Since snow and frozen soil are virtually absent on the Southern Great Plains, the initial values of these characteristics (at 0:00 on January 1, 1997) were set equal to zero at all the fields (without a significant error). As was noted above, a rough estimate of h_g can be used for a deep water table. For this reason, the initial values of this characteristic were set equal to 4 m at all the fields.

In contrast to the initial snow water equivalent and the water table depth, the initial soil moisture plays a certain role in finding solutions for the objects under study. Unfortunately, soil moisture data for the rooting zone and the soil layer beneath were not available for January 1, 1997. However, as was mentioned above, the moisture profiles in the rooting zone were measured on July 7 and 17, 1997, at field ER01 and on July 8 at field ER13 in El Reno. The condition that these values are equal to the rooting-zone humidity calculated for ER01 and ER13 on these days was used to obtain a unique solution to the problem for each field and to determine the corresponding initial soil moistures (the initial moisture was assumed to be the same for both model aeration layers). The soil moisture dynamics calculated for ER01 and ER13 have shown that this condition is satisfied when the initial volumetric soil moisture W_0 is equal to (W_{fc} – 0.035) at both fields (Fig. 3). Since no soil moisture data for the rooting zone and the soil layer beneath were available for CF01, CF02, LW02, and LW03, the initial moisture condition for these fields was approximated by that for ER01 and ER13, i.e., $W_0 = W_{fc}$. This approximation was based on the fact that, first, the objects under consideration were located relatively close to each other and, second, the effect of the initial soil water storage in the steppe zone usually vanishes in 2–3 months [36].

VERIFICATION RESULTS FOR THE SWAP MODEL

The calculations with the SWAP model for the fields chosen were carried out with a one-hour step from January 1 to December 31, 1997. According to the task of our study, we compared the observations with the modeled components of net radiation

$$R_n = R_S\downarrow - R_S\uparrow + R_L\downarrow - R_L\uparrow \quad (1)$$

and the heat balance

$$R_n = LE + H + G \quad (2)$$

Table 2. Comparison of the hourly net radiation and its components for three fields simulated by the SWAP model and measured at meteorological stations from January 1 to December 31, 1997

Field	Characteristic	Sample size	$\bar{x}_{obs}$, W m^{-2}	$\bar{\Delta}_{cal,\,obs}$, W m^{-2}	$RMSD_{cal,\,obs}$, W m^{-2}	*Ef*	*r*
LW02	$R_S\uparrow$	8321	36	5	14	0.92	0.99
	$R_L\uparrow$	8016	396	–10	22	0.87	0.95
	R_n	7913	75	7	29	0.98	0.99
ER01	$R_S\uparrow$	7879	36	5	14	0.93	0.99
	$R_L\uparrow$	7879	395	–15	24	0.85	0.96
	R_n	7879	75	12	23	0.99	1.00
CF01	$R_S\uparrow$	8713	38	4	12	0.95	0.99
	$R_L\uparrow$	8713	390	–9	18	0.91	0.97
	R_n	8713	79	9	24	0.99	1.00
Averages over three fields	$R_S\uparrow$	24913	36	5	13	0.93	0.99
	$R_L\uparrow$	24608	394	–11	21	0.88	0.96
	R_n	24505	77	9	25	0.98	1.00

at the land surface. Here, R_n is the net radiation, $R_S\downarrow$ and $R_L\downarrow$ are the short- and longwave radiation fluxes at the land surface, $R_S\uparrow$ is the reflected solar radiation, $R_L\uparrow$ is the longwave radiation of the land surface, G is the heat flux to the soil or snow cover, LE and H are the respective turbulent latent and sensible heat fluxes, E is the evapotranspiration from the land surface, and L is the latent heat of vaporization for water. Out of these characteristics, only $R_S\downarrow$ and $R_L\downarrow$ are specified in the model.

RADIATION CHARACTERISTICS

The calculated and observed hourly radiation-balance components for three grass-covered fields over all of 1997 are compared in Table 2. Specifically, Table 2 lists the averages $\bar{x}_{obs}$ of observed characteristics, the average systematic deviations $\bar{\Delta}_{cal,\,obs}$ and the rms deviations $RMSD_{cal,\,obs}$ of the calculated characteristics from the observed ones, the correlation coefficients *r*, and the efficiency *Ef* calculated according to [37] as

$$Ef = 1 - \frac{\sum_{\Omega}(x_{cal} - x_{obs})^2}{\sum_{\Omega}(x_{obs} - \bar{x}_{obs})^2}, \quad (3)$$

where x_{cal} and x_{obs} are the calculated and observed values of x and Ω is a discrete sample of x. If $Ef > 0.5$, the temporal dynamics of x is usually regarded as well reproduced by the model (if $Ef = 1$, the calculations should be thought of as ideal). If $Ef < 0$, the temporal variability of x is regarded as poorly reproduced (in which case even the simple average of the observed values is better than the calculated results).

It is evident from Table 2 that the SWAP model somewhat overestimates $R_S\uparrow$ and underestimates $R_L\uparrow$ as compared with the observations (ARM CART data). For example, the calculated hourly values of $R_S\uparrow$ averaged (over the year and the three fields) are 5 W m^{-2} (13%) higher than the corresponding observations, and the calculated values of $R_L\uparrow$ are 11 W m^{-2} (3%) lower than the observed ones; i.e., according to the model calculations, the heat loss of the land surface by this mechanism is less than in reality. Therefore, the overall net radiation of the land surface is somewhat overestimated (by 9 W m^{-2} or 12%). Nevertheless, the correlations between the calculated and observed values for all the characteristics and the calculated efficiency are very high ($r > 0.95$ and $Ef > 0.85$ in all the cases).

The systematic overestimation of the reflected solar radiation by the model can be attributed to the rather roughly specified albedo of grass, which was (on average) higher than the actual value. Recall that the albedo of grass in the model was set equal to a constant of 0.23, while the actual albedo exhibits an annual and diurnal cycle. Owing to the overestimated reflected radiation, the model produced a slightly underestimated longwave radiation of the land surface, which suggests that the model slightly underestimated the surface temperature.

For the intensive observation period, the calculated hourly values of R_n were compared with the corresponding data measured by various SGP97 participants at the six fields. Some of the results for grass and winter wheat are shown in Fig. 4, and their statistics are presented in Table 3 (no statistics are given for LW03, since the observation period there was too short—less than two days). Table 3 also compares the calculated R_n with the measurements performed at the Cyril and Lamont stations over the same observation period.

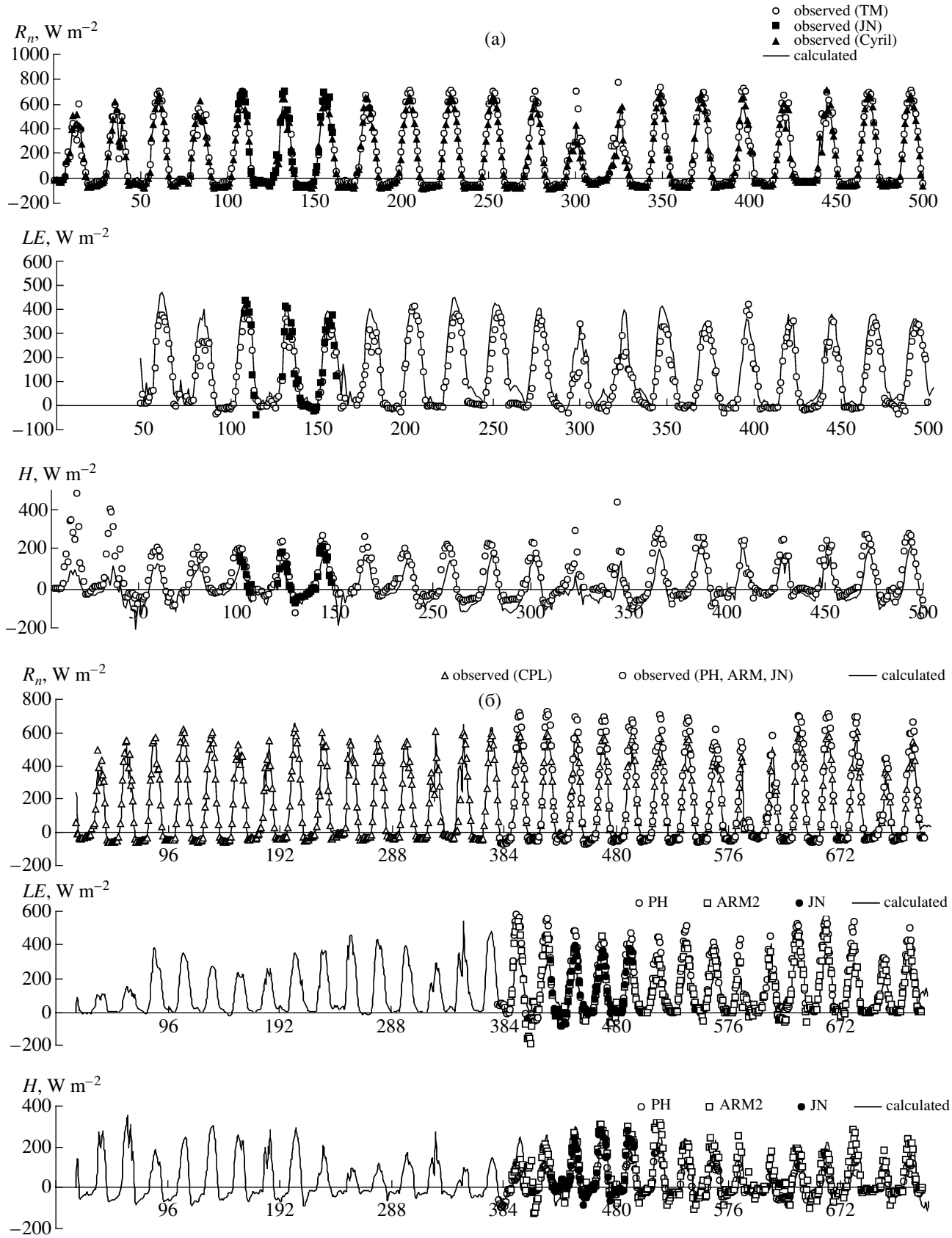

Fig. 4. Dynamics of the hourly R_n values simulated by the SWAP model and measured by various experiment participants and the turbulent latent LE and sensible H heat fluxes for (a) grass-covered field LW02 and (b) wheat-covered field CF02. The horizontal axis shows hours starting at (a) 0:30 of the 161st day and (b) 16:30 of the 167th day of the year 1997.

Table 3. Comparison of the hourly values of R_n, LE, and H simulated by the SWAP model at five fields and measured at the five fields by various experiment participants and at the Lamont and Cyril meteorological stations during the intensive observation period (see the notation in the text)

Field	Participant	Measuring technique for H and LE	R_n						Turbulent heat flux										
										LE					H				
			$N1$*	1**	2**	3**	Ef	r	$N2$*	1**	2**	3**	Ef	r	1**	2**	3**	Ef	r
LW02 (grass)	TM	EC	954	184	–22	75	0.92	0.98	875	125	24	54	0.83	0.94	52	–41	69	0.61	0.87
	JN	EC	56	231	–27	70	0.94	0.99	40	189	31	55	0.89	0.96	58	–26	38	0.82	0.95
	Cyril		762	155	6.7	38	0.98	1.00	–	–	–	–	–	–	–	–	–	–	–
ER01 (grass)	ARM	EBBR	1452	173	0	92	0.87	0.93	888	262	40	95	0.77	0.91	20	–34	73	–0.77	0.49
	CPL		68	169	–12	62	0.94	0.97	–	–	–	–	–	–	–	–	–	–	–
	PS	EBBR	627	182	–6	101	0.86	0.93	392	268	54	107	0.70	0.90	27	–60	91	–1.45	0.47
	JN	EC	64	201	–3	134	0.74	0.86	44	167	46	102	0.66	0.91	42	–47	75	–0.29	0.58
	JPBK	EC	703	193	–21	91	0.90	0.96	547	198	37	79	0.87	0.96	18	–70	90	–1.07	0.59
	PH	EC	478	188	–13	84	0.91	0.96	406	185	23	67	0.87	0.97	0	–41	69	–0.03	0.64
	Cyril		1019	147	16	25	0.99	1.00	–	–	–	–	–	–	–	–	–	–	–
CF01 (grass)	ARM	EC	1425	165	–2	65	0.93	0.974	877	212	43	85	0.76	0.91	61	–48	69	0.02	0.73
	Lamont	EC	1494	150	13	32	0.98	1.00	–	–	–	–	–	–	–	–	–	–	–
ER13 (winter wheat)	JPBK	EC	621	178	–26	104	0.85	0.94	492	101	0	76	0.66	0.81	78	–25	73	0.68	0.85
	JN	EC	143	198	–29	96	0.89	0.97	136	142	–32	74	0.78	0.92	48	3	57	0.71	0.86
CF02 (winter wheat)	CPL		736	152	9	37	0.97	0.99	–	–	–	–	–	–	–	–	–	–	–
	PH	EC	378	177	–22	75	0.92	0.99	365	155	–53	100	0.70	0.93	26	17	50	0.37	0.93
	ARM	EC	378	177	–22	75	0.92	0.99	351	128	–21	68	0.80	0.92	65	–16	45	0.81	0.92
	JN	EC	378	177	–22	75	0.92	0.99	72	125	–41	77	0.73	0.96	77	–11	36	0.89	0.95
Weighted averages	over 5 fields		7705	176	–9	80	0.90	0.96	5485	184	21	80	0.78	0.92	41	–37	70	–0.06	0.72
	over 3 grass fields		5827	178	–9	83	0.90	0.96	4069	204	36	80	0.80	0.93	35	–47	74	–0.31	0.66
	over 2 winter wheat fields		1878	169	–11	71	0.91	0.97	1416	127	–24	80	0.72	0.89	58	–8	57	0.64	0.89
	over stations		3275	150	13	31	0.98	1.00	–	–	–	–	–	–	–	–	–	–	–

* $N1$ is the sample size in the measurements of R_n, $N2$ is the sample size in the measurements of LE and H; ** 1, $\bar{x}_{\text{obs}}$; 2, $\bar{\Delta}_{\text{cal, obs}}$; and 3, $RMSD_{\text{cal, obs}}$, all in W m^{-2}. The acronyms in the second column correspond to the names of experiment participants and their institutions: ARM is the DOE Atmosphere and Radiation Measurement Program, CPL is Christa Peters (Lidard, Georgia Tech.), JN is John Norman (University of Wisconsin, Madison), JPBK is John Prueger and Bill Kustas (USDA Agricultural Research Service), PH is Paul Houser (NASA Goddard Space Flight Center), PS is Patrick Starks (USDA, Agricultural Research Service), and TM is Tilden Meyers (NOAA Air Resources Laboratory Atmospheric Turbulence and Diffusion Division).

Table 4. Pairwise comparison of the hourly values of R_n, LE, and H measured by various SGP97 participants at the same field

Characteristic	Field	Participant		Sample size	Mean $\bar{x}_1$, W m^{-2}	Mean $\bar{x}_2$, W m^{-2}	$\bar{\Delta}_{obs} = (\overline{x_2 - x_1})$, W m^{-2}	$RMSD_{obs}$, W m^{-2}
		1	2					
R_n	ER01 (grass)	ARM	JPBK	627	188	193	5	20
		ARM	PS	703	179	182	3	8
		PS	JPBK	514	189	192	3	17
		JPBK	PH	348	188	190	2	17
		ARM	PH	478	180	188	8	16
		Mean		2670	184	189	4	15
	CF02 (winter wheat)	PH	CPL	373	175	147	–28	56
LE	ER01 (grass)	ARM	JPBK	339	321	316	–5	43
		ARM	PS	383	277	275	–3	44
		PS	JPBK	267	299	299	–1	34
		JPBK	PH	192	211	225	14	46
		ARM	PH	250	280	283	3	52
		Mean		1431	283	284	0.5	43
	CF02 (winter wheat)	PH	ARM	343	161	126	–34	59
H	ER01 (grass)	ARM	JPBK	339	20	44	25	52
		ARM	PS	383	19	28	9	45
		PS	JPBK	267	31	44	13	36
		JPBK	PH	192	20	1	–19	40
		ARM	PH	250	18	28	10	58
		Mean		1431	21	31	10	47
	CF02 (winter wheat)	PH	ARM	343	29	64	35	59

Interestingly, a comparison of the calculated R_n with the station observations reveals systematic overestimation ($\bar{\Delta}_{cal,\,obs} > 0$) of the net radiation (by 13 W m^{-2} or 8% on average), while a comparison with the field measurements shows an inverse pattern, namely, systematic underestimation ($\bar{\Delta}_{cal,\,obs} < 0$) of the calculated R_n (by 9 W m^{-2} or 5% on average). This suggests that the field and station measurements differ significantly: the values of R_n obtained at all the fields are higher (on average by 25 W m^{-2}) than those measured at the stations. These large discrepancies are caused primarily by the different methods used for net radiation measurements: net radiometers were used for field measurements of R_n, while at the stations it was calculated from measurements of all four components [see Eq. (1)]. Moreover, the fact that the fields were some distance from the stations and the differences in the type of the land surface could also affect the results. However, it seems that the influence of the last two factors is insignificant, since (i) the measurements in all cases were conducted over grass and (ii) insignificant differences were found between the net radiations measured at Cyril and Lamont, which are much farther apart than the distance from them to the fields (the annual mean R_n is 75 W m^{-2} at Cyril and 79 W m^{-2} at Lamont).

Since the input data for the model included station measurements of incoming short- and longwave radiation, discrepancies between the model results for the fields and the field measurements are unavoidable. Note that the $RMSD_{cal,\,obs}$ values derived from the field measurements of R_n (Table 3) are comparable with the rms deviations $RMSD_{obs}$ of the field measurements of R_n from the station measurements: the values of $RMSD_{obs}$ vary from 44 to 102 W m^{-2} and average 74 W m^{-2}, while the values of $RMSD_{cal,\,obs}$ vary from 37 to 134 W m^{-2} (and average 80 W m^{-2}). The calculation efficiency and the correlation coefficient are very high and average 0.90 and 0.96, respectively (Table 3).

When the station observations rather than the field measurements are used for model verification, the values of $RMSD_{cal,\,obs}$ decrease by more than half, on average down to 31 W m^{-2} (Table 3), and become comparable with the discrepancies between the measurements of $RMSD_{obs}$ made by various experiment participants at the same field (Table 4). It is evident from Table 4 that, for field ER01, where the observations were most intensive, the values of $RMSD_{obs}$ between different series of measured R_n vary from 8 to 20 W m^{-2} (15 W m^{-2} on average). These differences can be caused by the different measurement techniques and the local spatial inhomogeneity of the fields.

Table 5. Comparison of the hourly heat fluxes *G* into the soil averaged over the intensive observation period as simulated by the SWAP model ($\bar{x}_{cal}$) and measured by various SGP97 participants ($\bar{x}_{obs}$) at five fields

Field	Participant	Sample size	$\bar{x}_{obs}$, W m^{-2}	$\bar{x}_{cal}$, W m^{-2}	$\bar{\Delta}_{cal,\,obs}$, W m^{-2}
LW02	TM	954	15.9	6.7	–9.2
	JN	56	30.8	7.3	–23.5
ER01	ARM	1452	7.1	6.5	–0.6
	CPL	68	8.0	7.3	–0.7
	PS	648	6.3	6.4	0.1
	JN	64	12.6	7.3	–5.3
	JPBK	703	–1.3	6.7	8.0
	PH	478	6.7	7.1	0.4
ER13	JPBK	143	11.7	6.7	–5.0
	JN	621	9.0	6.6	–2.4
CF01	ARM	1425	8.1	7.0	–1.1
CF02	CPL	374	–5.9	6.7	12.6
	PH, ARM, JN	729	2.9	7.1	4.2
Weighted average over the fields			7.0	6.8	–0.2

The differences between the reproduced R_n for fields with grass and winter wheat are insignificant (Table 3). Averaged over the corresponding fields, the values of $RMSD_{cal,\,obs}$ are equal to 83 and 71 W m^{-2}, Ef = 0.90 and 0.91, and r = 0.96 and 0.97 for grass and wheat, respectively.

The analysis above suggests that the SWAP model reproduces rather well the diurnal and annual cycles of the net radiation at the land surface covered with grass and winter wheat. The resulting calculation "errors" are caused, in many respects, by uncertainties in the measurements used for comparison with the model results and for model initialization.

Turbulent Latent Heat Flux

Some results of comparison of the fluxes *LE* simulated by the model and field measurements are presented in Fig. 4, and the statistics of the results are given in Table 3.

An analysis of the results shows that the total evaporation *E* in the model is somewhat overestimated ($\bar{\Delta}_{cal,\,obs} > 0$) for grassland sites and is underestimated ($\bar{\Delta}_{cal,\,obs} < 0$) for wheat-covered sites as compared with the measurements (Table 3): the model values of *LE* over all three fields are higher than the observations by 36 W m^{-2} (18%) on average for grass and are lower than the observations by 24 W m^{-2} (19%) on average for winter wheat. These systematic deviations can be caused, to a high degree, by the inaccurately specified LAI and LSAI. The other statistical characteristics for the comparison of the calculated and observed *LE* for grass and wheat differ little: on average, $RMSD_{cal,\,obs}$ = 80 W m^{-2}, Ef = 80, and r = 0.93 for grass; and $RMSD_{cal,\,obs}$ = 80 W m^{-2}, Ef = 0.72, and r = 0.89 for winter wheat. The high values of Ef testify to the ability of the SWAP model to reproduce the time variability of *LE*.

To understand how significant the resulting $\bar{\Delta}_{cal,\,obs}$ and $RMSD_{cal,\,obs}$ are in comparison with the scatter in the *LE* measurements, Table 4 gives pairwise comparisons of the *LE* fluxes measured simultaneously by various SGP97 participants at the same field. For grass fields, the systematic differences between the measurements can be considered small (about 0.5 W m^{-2} on average), while for wheat-covered sites, the values of *LE* measured at CF02 by two research groups differ on average by 34 W m^{-2}, which even somewhat exceeds the systematic deviation of the calculated values from the observed ones (equal to 24 W m^{-2}). The values of $RMSD_{obs}$ for various measured series of *LE* average 43 W m^{-2} for grass and can reach 59 W m^{-2} for winter wheat. Thus, the $RMSD_{cal,\,obs}$ values for *LE* exceed $RMSD_{obs}$ less than twofold on average.

Turbulent Sensible Heat Flux

Some of the results for the dynamics of the sensible heat flux *H* reproduced by the SWAP model are shown in Fig. 4 and are summarized in Table 3. Averaged over all fields, the calculated values of *H* are underestimated by 37 W m^{-2} as compared to the observations, which should be expected because of the overestimated model values of *LE*. However, the calculated and observed sensible heat fluxes for winter wheat sites agree much better than those for grass sites (Table 3). On average, $\bar{\Delta}_{cal,\,obs}$ = –8 W m^{-2}, $RMSD_{cal,\,obs}$ = 57 W m^{-2}, r = 0.89, and Ef = 0.64 for wheat sites. Note that $RMSD_{cal,\,obs}$ is virtually the same as the discrepancy between the two series of simultaneous measurements of *H* made at CF02 ($RMSD_{obs}$ = 59 W m^{-2}) (Table 4).

For grass fields, the best results were obtained for LW02 (Ef > 0.6) (Fig. 4a, Table 3), and the worst results were obtained for ER01 (Table 3), the same as with *LE*. On average, $\bar{\Delta}_{cal,\,obs}$ = –47 W m^{-2}, $RMSD_{cal,\,obs}$ = 74 W m^{-2}, r = 0.66, and Ef < 0 for grassland sites. It should be noted that an analysis of *H* measured simultaneously by various SGP97 participants at the grass field ER01 revealed rather large discrepancies between them (Table 4): the discrepancies between the means and the rms deviations reach 25 and 58 W m^{-2}, respectively (and their averages are 10 and 47 W m^{-2}, respec-

tively). In connection with these uncertainties in the measured data, the rms deviations of the calculated and observed values of H for ER01 (varying from 69 to 91 W m^{-2}) can be viewed as satisfactory. We believe that the systematic error in the calculated H (and in the other heat balance components) could be reduced if more accurate data on LAI and LSAI were available.

Heat Flux to the Soil

Since the heat flux G to the soil in the warm period of the year is less than R_n by approximately one order of magnitude [38], the contribution of the former to heat balance formation at the land surface can be considered insignificant. For this reason, the warm-period parametrization of G in the SWAP model is based on approximate empirical dependences derived from generalized global estimates for the annual cycle of soil heat transfer [39]. As a result, the SWAP model has no diurnal cycle of G. Thus, it seems reasonable to analyze the reproduced soil heat transfer averaged over observation periods.

Averaged over the corresponding observation periods, the hourly fluxes G measured by various SGP97 participants and simulated by the SWAP model for five fields are listed in Table 5. An analysis of these results suggests the following conclusions. First, despite the very rough parametrization of G in the SWAP model, the averages of the observed and simulated G are rather close to each other: averaged over all the fields, the observed flux G is 7.0 W m^{-2} and the simulated flux is 6.8 W m^{-2}. Second, the observed fluxes G themselves are very small and average less than 5% of the corresponding observed net radiation R_n. These findings suggest that the contribution of the error in the calculated G to the final result is insignificant, which justifies the simplified parametrization of G used in the model.

CONCLUSIONS

The unique observations obtained over the Southern Great Plains during the SGP97 experiment have been used to validate the SWAP model. Specifically, the hourly measurements of the net radiation and its components, the heat flux to the soil, and turbulent fluxes of heat and water vapor at six fields covered with grass and winter wheat were used for model validation. The rms deviations of the simulated characteristics from the field measurements made during the intensive observation period average 80 W m^{-2} for the net radiation, 80 W m^{-2} for latent heat fluxes, and 70 W m^{-2} for sensible heat fluxes. An analysis of the measurements used for model initialization and comparison with model results showed that the deviations of the simulated magnitudes from the observed ones are caused mainly by the uncertainties in the measurements themselves. For example, the rms deviations between series of simultaneous measurements made by various SGP97 participants at the same field were found to be 20, 46, and 49 W m^{-2} for R_n, LE, and H, respectively. Moreover, the initial radiation data (incoming short- and longwave radiation) required for conducting model calculations for fields were collected not at these fields but rather at the nearest ARM CART stations, while the initial meteorological characteristics (precipitation and wind speed and air temperature, humidity, and pressure) were measured at nearby Oklahoma Mesonet stations. In view of the differences in these sites, unavoidable errors had to appear in the calculation results. For the same reason and because of the differences in the measuring techniques, the net radiations R_n measured at the fields and ARM CART stations have widely varying magnitudes: the rms deviations for them average 74 W m^{-2}, which is comparable with the above rms deviations of the calculated net radiation from field observations (80 W m^{-2}). It should be noted that the initial meteorological data, model parameters, and initial conditions also introduced a number of uncertainties related to missed meteorological measurements and the lack of data on the initial soil moisture and the annual dynamics of phenological and phytometric vegetation characteristics.

The analysis performed suggests that the SWAP model (in the absence of any calibration of its parameters) reproduces quite well the dynamics of land-surface heat and moisture exchange with the atmosphere in steppe ecosystems (both natural and agricultural) located in continental semiarid regions. This makes it possible to use the model for hydrological, climatic, and ecological studies in such regions.

ACKNOWLEDGMENTS

This work was supported by the Russian Foundation for Basic Research, project no. 02-05-64213.

REFERENCES

1. E. M. Gusev, *Formation of the Regime and Resources of Soil Waters in the Winter–Spring Period* (Nauka, Moscow, 1993) [in Russian].
2. J. Polcher, The Global Land–Atmosphere System Study (GLASS), GEWEX News **11** (2), 5–6 (2002).
3. E. M. Gusev and O. N. Nasonova, "Parametrization of Heat and Water Exchange on Land Surface for Coupling Hydrologic and Climate Models," Vodn. Resur. **25**, 421–431 (1998).
4. E. M. Gusev and O. N. Nasonova, "Parametrization of Heat and Moisture Exchange between the Land Surface and the Atmosphere," in *Water Problems at the Turn of the Century* (Nauka, Moscow, 1999), pp. 152–171 [in Russian].
5. E. M. Gusev and O. N. Nasonova, "Modeling of Heat and Water Exchange on the Land Surface on a Regional Scale," Vodn. Resur. **27**, 32–47 (2000).

6. E. M. Gusev and O. N. Nasonova, "Parametrization of Heat and Moisture Transfer in the Ground Waters–Soil–Plant/Snow Cover–Atmosphere System for Territories with a Continental Climate," Pochvovedenie, No. 6, 733–747 (2000).
7. E. M. Gusev, and O. N. Nasonova, "Parametrization of Heat and Moisture Transfer Processes in Ecosystems of Boreal Forests," Izv. Akad. Nauk, Fiz. Atmos. Okeana **37**, 182–200 (2001) [Izv., Atmos. Ocean. Phys. **37**, 167–185 (2001).
8. A. Boone, F. Habets, J. Noilhan, *et al.*, The Rhone-Aggregation Land Surface Scheme Intercomparison Project: An Overview, J. Clim. **17**, 187–208 (2004).
9. T. H. Chen, A. Henderson-Sellers, P. C. D. Milly, *et al.*, Cabauw? Experimental Results from the Project for Intercomparison of Land-Surface Parameterization Schemes, J. Clim. **10**, 1194–1215 (1997).
10. Ye. M. Gusev and O. N. Nasonova, The Land Surface Parameterization Scheme SWAP: Description and Partial Validation, Global Plan. Change, **19** (1–4), 63–86 (1998).
11. Ye. M. Gusev and O. N. Nasonova, The Land Surface Parameterization Scheme SWAP: Description and Validation, IAHS Publ., No. 254, 113–122 (1999).
12. Ye. M. Gusev and O. N. Nasonova, An Experience of Modelling Heat and Water Exchange at the Land Surface on a Large River Basin Scale, J. Hydrol. **233** (1–4), 1–18 (2000).
13. Ye. M. Gusev and O. N. Nasonova, The Simulation of Heat and Water Exchange at the Land–Atmosphere Interface for the Boreal Grassland by the Land-Surface Model SWAP, Hydrolog. Proc. **16**, 1893–1919 (2002).
14. X. Liang, E. F. Wood, D. P. Lettenmaier, *et al.*, The Project for Intercomparison of Land-Surface Parameterization Schemes (PILPS) Phase-2(c) Red-Arkansas River Basin Experiment: 2. Spatial and Temporal Analysis of Energy Fluxes, Global Plan. Change **19** (1–4), 137–159 (1998).
15. D. Lohmann, D. P. Lettenmaier, X. Liang, *et al.*, The Project for Intercomparison of Land-Surface Parameterization Schemes (PILPS) Phase-2(c) Red-Arkansas River Basin Experiment: 3. Spatial and Temporal Analysis of Water Fluxes, Global Plan. Change **19** (1–4), 161–179 (1998).
16. C. A. Schlosser, A. G. Slater, A. Robock, *et al.*, Simulations of a Boreal Grassland Hydrology at Valdai, Russia: PILPS Phase 2(d), Mon. Weather Rev. **128**, 301–321 (2000).
17. A. G. Slater, C. A. Schlosser, C. E. Desborough, *et al.*, The Representation of Snow in Land Surface Schemes: Results from PILPS 2(d), J. Hydrometeorol. **2**, 7–25 (2001).
18. E. F. Wood, D. P. Lettenmaier, X. Liang, *et al.*, The Project for Intercomparison of Land-Surface Parameterization Schemes (PILPS) Phase-2(c) Red-Arkansas River Basin Experiment: 1. Experiment Description and Summary Intercomparisons, Global Plan. Change **19** (1–4), 115–135 (1998).
19. A. I. Budagovskii, "Principles of the Method of Calculating the Duty of Water and Irrigation Regimes," Vodn. Resur. **16**, 38–48 (1989).
20. S. S. Zilitinkevich, *Dynamics of the Atmospheric Boundary Layer* (Gidrometeoizdat, Leningrad, 1970) [in Russian].
21. S. S. Zilitinkevich and A. S. Monin, *Turbulence in Dynamic Atmospheric Models* (Nauka, Leningrad, 1971) [in Russian].
22. W. H. Green and G. A. Ampt, Studies' on Soil Physics. 1. The Flow of Air and Water through Soils, J. Agr. Sci. **4**, 1–24 (1911).
23. J. M. Schneider and D. K. Fisher, Meeting GEWEX/GCIP Measurement Needs by Adding Automated Measurements of Soil Water and Temperature Profiles to the DOE ARM/CART Southern Great Plains Site, *Preprint of AMS 13th Conference on Hydrology*, pp. 265–268 (1997).
24. R. B. Clapp and G. M. Hornberger, Empirical Equations for Some Soil Hydraulic Properties, Water Resour. Res. **14**, 601–604 (1978).
25. F. J. Leij, W. J. Alves, and M. Th. van Genuchten, The UNSODA Unsaturated Soil Hydraulic Database, in *Proceedings of the International Workshop on Characterization and Measurement of the Hydraulic Properties of Unsaturated Porous Media* (UCR, Riverside, California, 1999).
26. M. G. Schaap, F. J. Leij, and M. Th. van Genuchten, Neural Network Analysis for Hierarchical Prediction of Soil Water Retention and Saturated Hydraulic Conductivity, Soil Sci. Soc. Am. J. **62**, 847–855 (1998).
27. M. Th. van Genuchten, A Closed-Form Equation for Predicting the Hydraulic Conductivity of Unsaturated Soils, Soil Sci. Soc. Am. J. **44**, 892–898 (1980).
28. *Practical Course on Soil Science*, Ed. by I. S. Kaurichev (Kolos, Moscow, 1980) [in Russian].
29. J. Simunek, K. Huang, M. Sejna, *et al.*, The HYDRUS-ET Software Package for Simulating the One-Dimensional Movement of Water, Heat and Multiple Solutes in Variably Saturated Media. Version 1.1 (Institute of Hydrology SAV, Bratislava, 1997).
30. E. M. Gusev and O. E. Busarova, "Modeling the Leaf Area Index Dynamics of Agricultural Vegetation," Meteorol. Gidrol., No. 1, 100–107 (1998).
31. N. N. Vygodskaya and I. I. Gorshkova, *Theory and Experiment in Remote Studies of Vegetation* (Gidrometeoizdat, Leningrad, 1987) [in Russian].
32. V. L. Gaevskii, "On the Role of Albedo in Forming the Radiation Regime of the Surface," Trudy Gl. Geofiz. Observ., No. 39 (100), 150–163 (1953).
33. N. A. Danilova, "Evapotranspiration from Fields of Winter and Summer Crops over the Vegetation Period," in *Heat and Radiation Balance of the Natural Vegetation and Agricultural Fields* (Nauka, Moscow, 1965), pp. 117–126 [in Russian].
34. B. P. Mohanty, T. H. Skaggs, and J. S. Famiglietti, Analysis and Mapping of Field-Scale Soil Moisture Variability Using High-Resolution, Ground-Based Data during

the Southern Great Plains 1997 (SPG97) Hydrology Experiment, Water Resour. Res. **36**, 1023–1031 (2000).

35. B. P. Mohanty, P. J. Shouse, D. A. Miller, and M. Th. van Genuchten, Soil Property Database—Southern Great Plains, 1997 Hydrology Experiment, Water Resour. Res. **38** (5) (2002).
36. Ye. M. Gusev, O. Ye. Busarova, and O. N. Nasonova, Modelling Soil Water Dynamics and Evapotranspiration for Heterogeneous Surfaces of the Steppe and Forest-Steppe Zones on Regional Scale, J. Hydrol. **206** (3–4), 281–297 (1998).
37. J. E. Nash and J. V. Sutcliffe, River Flow Forecasting through Conceptual Models: 1. A Discussion of Principles, J. Hydrol. (Amsterdam) **10**, 282–290 (1970).
38. A. V. Pavlov, *Thermal Physics of Landscapes* (Nauka, Novosibirsk, 1979) [in Russian].
39. M. I. Budyko, *Heat Balance of the Earth's Surface* (Gidrometeoizdat, Leningrad, 1956) [in Russian].

Translated by I. Ruzanova